# Pros and Cons of Rotating Ground Motion Records to Fault-Normal/Parallel Directions for Response History Analysis of Buildings

Erol Kalkan, M.ASCE[1]; and Neal S. Kwong[2]

**Abstract:** According to the regulatory building codes in the United States (e.g., 2010 California Building Code), at least two horizontal ground motion components are required for three-dimensional (3D) response history analysis (RHA) of building structures. For sites within 5 km of an active fault, these records should be rotated to fault-normal/fault-parallel (FN/FP) directions, and two RHAs should be performed separately (when FN and then FP are aligned with the transverse direction of the structural axes). It is assumed that this approach will lead to two sets of responses that envelope the range of possible responses over all nonredundant rotation angles. This assumption is examined here, for the first time, using a 3D computer model of a six-story reinforced-concrete instrumented building subjected to an ensemble of bidirectional near-fault ground motions. Peak values of engineering demand parameters (EDPs) were computed for rotation angles ranging from 0 through 180° to quantify the difference between peak values of EDPs over all rotation angles and those due to FN/FP direction rotated motions. It is demonstrated that rotating ground motions to FN/FP directions (1) does not always lead to the maximum responses over all angles, (2) does not always envelope the range of possible responses, and (3) does not provide maximum responses for all EDPs simultaneously even if it provides a maximum response for a specific EDP. **DOI: [10.1061/(ASCE)ST.1943-541X.0000845](https://doi.org/10.1061/(ASCE)ST.1943-541X.0000845).** © 2013 American Society of Civil Engineers.

**Author keywords:** Near-fault ground motion; Directivity; Response history analysis; Seismic effects.

## Introduction

In the United States, both the California Building Code [International Conference for Building Officials (ICBO) 2010] and International Building Code (ICBO 2009) refer to Chapter 16 of ASCE/SEI-7 (ASCE 2010) when response history analysis (RHA) is required for design verification of building structures. For three-dimensional (3D) analyses of symmetric-plan buildings, ASCE/SEI-7 requires either spectrally matched or intensity-based scaled ground motion records, which consist of pairs of appropriate horizontal ground acceleration components. For each pair of horizontal components, a square-root-of-sum-of-squares (SRSS) spectrum shall be constructed by taking the SRSS of the 5% damped response spectra of the unscaled components. Each pair of motions shall then be scaled with the same scale factor such that the mean of the SRSS spectra does not fall below the corresponding ordinate of the target spectrum in the period range from $0.2T_1$ to $1.5T_1$ (where $T_1$ is the elastic first-mode vibration period of the structure). The design value of an engineering demand parameter (EDP)—member forces, member deformations, or story drifts—shall then be taken as the mean value of the EDP over seven (or more) ground motion pairs, or its maximum value over all ground motion pairs if the system is analyzed for fewer than seven ground motion pairs. This procedure requires a minimum of three records.

[1]Research Structural Engineer, USGS, Menlo Park, CA 94025 (corresponding author). E-mail: ekalkan@usgs.gov

[2]Ph.D. Candidate, Univ. of California, Berkeley, CA 94709. E-mail: nealsimonkwong@berkeley.edu

As input for RHAs, strong motion networks provide users with ground accelerations recorded in three orthogonal directions—two horizontal and one vertical. The sensors recording horizontal accelerations are often, but not always, oriented in the north-south (N-S) and east-west (E-W) directions. These records with station-specific orientations are referred to as as-recorded ground motions. If the recording instrument was installed in a different orientation about the vertical axis than the N-S and E-W directions, and the corresponding pair of ground motions was of interest, then a two-dimensional (2D) rotation transformation can be applied to the as-recorded motion. Since the instrument could have been installed at any angle, the rotated versions are possible realizations.

Although the as-recorded pair of ground motion may be applied to the structural axes corresponding to the structure's transverse and longitudinal directions, there is no reason why the pair should not be applied to any other axes rotated about the structural vertical axis. Equivalently, there is no reason why rotated versions should not be applied to the structural axes. Which angle, then, should one select for RHA remains a question in earthquake engineering practice.

This notion of rotating ground motion pairs has been studied in various contexts. According to Penzien and Watabe (1975), the principal axis of a pair of ground motions is the angle or axis at which the two horizontal components are uncorrelated. Using this idea of principal axis, the effects of seismic rotation angle, defined as the angle between the principal axes of the ground motion pair and the structural axes, on structural response was investigated (Franklin and Volker 1982; Fernandez-Davila et al. 2000; MacRae and Mattheis 2000; Tezcan and Alhan 2001; Khoshnoudian and Poursha 2004; Rigato and Medina 2007; Lagaros 2010; Goda 2012). A formula for deriving the angle that yields the peak elastic response over all possible nonredundant angles, called $\theta_{\text{critical}}$ (or $\theta_{\text{critical}}$), was proposed by Wilson et al. (1995). Other researchers have improved upon the closed-form solution of

Wilson et al. (1995) by accounting for the statistical correlation of horizontal components of ground motion in an explicit way (Lopez and Torres 1997; Lopez et al. 2000). The Wilson et al. (1995) formula is, however, based on concepts from response spectrum analysis—an approximate procedure used to estimate structural responses in the linear-elastic domain. Focusing on linear-elastic, multi-degree-of-freedom symmetric, and asymmetric structures, Athanatopoulou (2005) investigated the effect of the rotation angle on structural response using RHAs and provided formulas for determining the maximum response over all rotation angles, given the response histories for two orthogonal orientations. Athanatopoulou (2005) also concluded that the critical angle corresponding to peak response over all angles varied not only with the ground motion pair under consideration but with the response quantity of interest as well.

According to Section 1615A.1.25 of the California Building Code (ICBO 2010), at sites within 3 mi (5 km) of the active fault that dominates a hazard, each pair of ground motion components shall be rotated to the fault-normal (FN) and fault-parallel (FP) directions (also called strike-normal and strike-parallel directions) for 3D RHAs. It is believed that the angle corresponding to the FN/FP directions will lead to the most critical structural response. This assumption is based on the fact that, in the proximity of an active fault system, ground motions are significantly affected by the faulting mechanism, direction of rupture propagation relative to the site, and the possible static deformation of the ground surface associated with fling-step effects (Bray and Rodriguez-Marek 2004; Kalkan and Kunnath 2006). These near-source effects cause most of the seismic energy from the rupture to arrive in a single, coherent, long-period pulse of motion in the FN/FP directions (Mavroeidis and Papageorgiou 2003; Kalkan and Kunnath 2007, 2008). Thus, rotating ground motion pairs to FN/FP directions is assumed to be a conservative approach appropriate for design verification of new structures or performance evaluation of existing structures.

Using a 3D structural model of an instrumented building and an ensemble of near-fault ground motion records, this study systematically evaluates whether FN/FP directions rotated ground motions lead to conservative (the term conservative is used here either with peak or close to peak EDP values) estimates of EDPs from RHAs.

## Description of Structural System and Computer Model

The testbed system used is a 3D computer model of the former Imperial County Services building in El Centro, California. This relatively symmetrical building had an open first story and five occupied stories (Fig. 1). Designed in 1968, its vertical load carrying system consisted of 12.7 cm reinforced concrete (RC) thick slabs supported by RC pan joists, which in turn were supported by RC frames spanning in the orthogonal direction. Fig. 2 shows the foundation and typical floor layouts. The lateral resistance of all levels in the longitudinal (E-W) direction was provided by two exterior moment frames at Column Lines 1 and 4 and two interior moment frames on Column Lines 2 and 3. The lateral resistance in the transverse (N-S) direction was not continuous. At the ground floor level, it was provided by four short shear walls located along Column Lines A, C, D, and E and extending between Column Lines 2 and 3 only (Fig. 2, top). At the second floor and above, lateral (N-S) resistance was provided by two shear walls at the east and west ends of the building. This caused the building to be top heavy with a soft first story, as shown in Fig. 1 (Todorovska and Trifunac 2008). The design strength of the concrete was 34.5 MPa for columns, 20.7 MPa for the elements below ground level, and 27.6 MPa elsewhere. All reinforcing steel was specified to be grade 40 ($Fy = 276$ MPa). The foundation system consisted of piles under each column with pile caps connected with RC beams (Fig. 2 top).

The building was instrumented in 1976 with 13 sensors at 4 levels of the building and 3 sensors at a free-field site. The sensors in the building measure horizontal accelerations at the ground floor, second floor, fourth floor, and roof; vertical acceleration was measured at the ground floor; the instrumentation layout of the building is given in Kalkan and Kwong (2012). The recorded motions of this building are available only for the Mw6.5 1979 Imperial Valley earthquake, during which this building was damaged and subsequently demolished. The peak recorded accelerations during this earthquake were 0.34 g at the ground floor and 0.58 g at the roof level. This building is a rare case of an instrumented building severely damaged by an earthquake (Goel and Chadwell 2007).
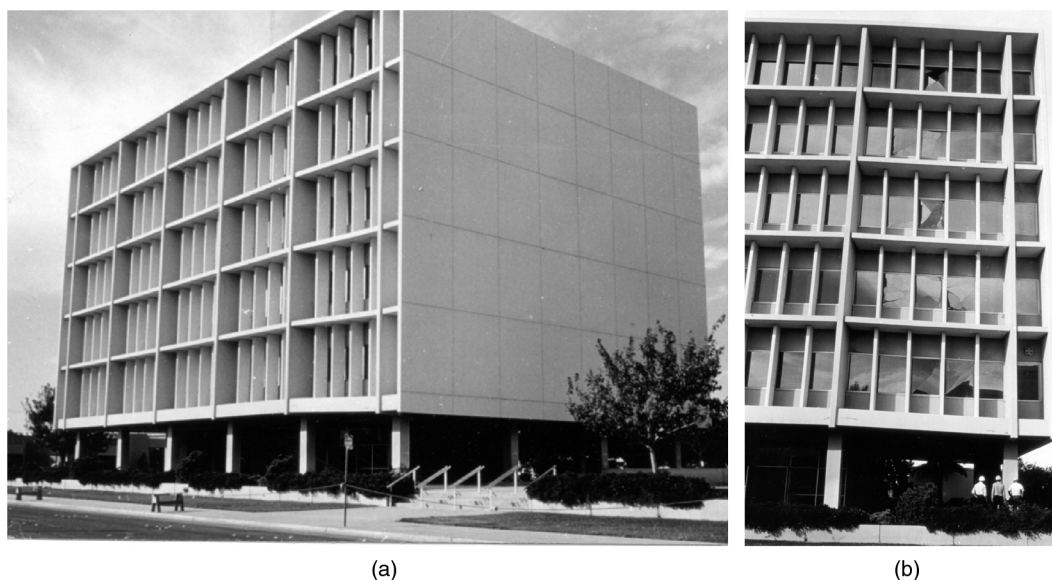


**Fig. 1.** (a) Imperial County Services building (photograph by C. Rojahn, with permission from USGS); (b) east end of Imperial County Services building, showing a row of columns (far right) that failed during main shock; view is north (photograph by C. Rojahn, with permission from USGS)
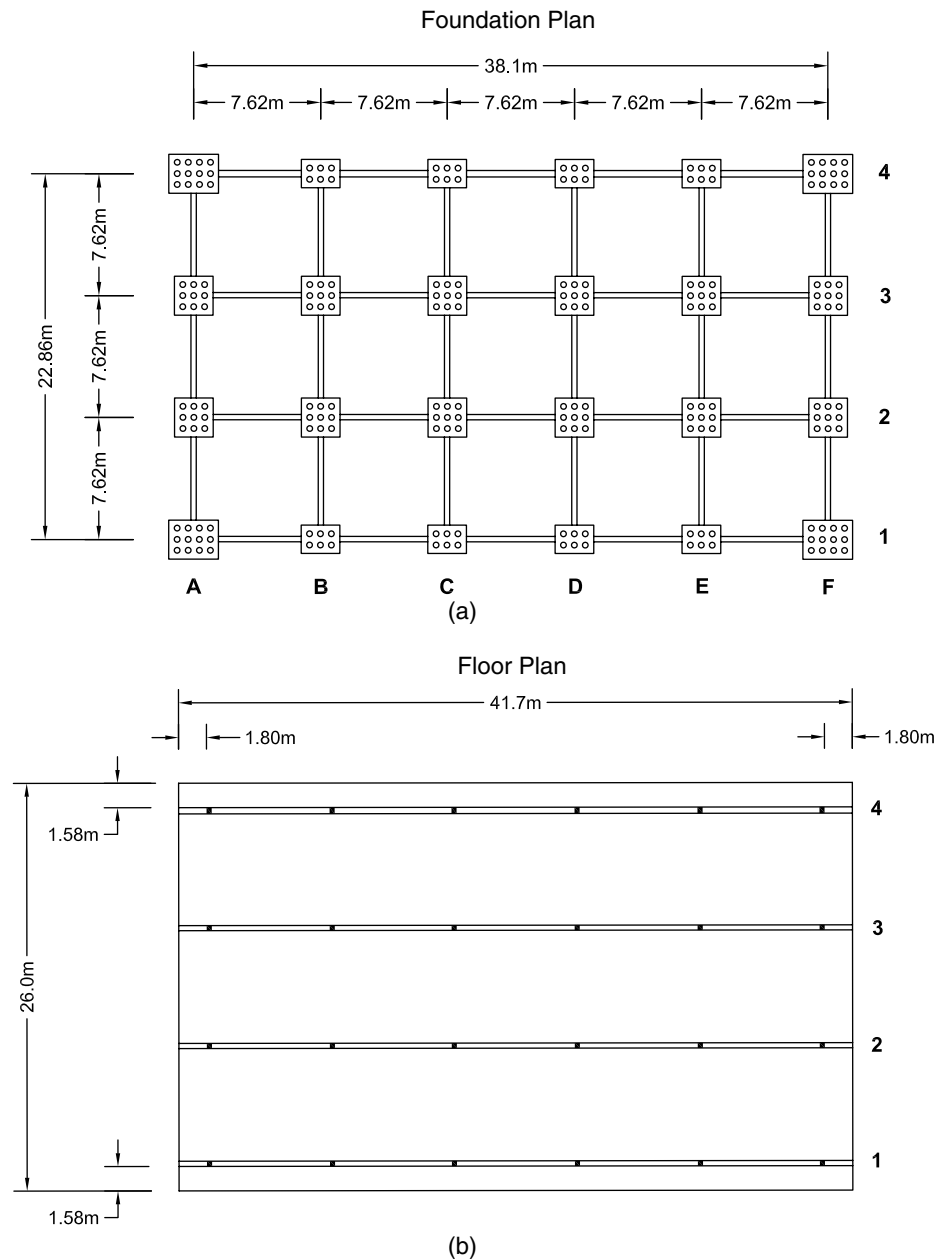
## Foundation Plan



(a)

## Floor Plan



(b)

**Fig. 2.** Foundation and ground-level plan and typical floor layout of Imperial County Services building. Note: Transverse (Y or north-south) and longitudinal (X or east-west)

Fig. 1 (bottom) shows the concentration of damage in the ground floor columns as a result of concrete spalling and buckling of reinforcing bars. The details about the design, recorded data, and observed damage can be found in Kojic et al. (1984).

The 3D computer model of this building was created using OpenSees (2010). Centerline dimensions were used in the element modeling, the composite action of floor slabs was not considered, and the columns were assumed to be fixed at the base level. For the response history evaluations, masses were applied to frame models based on the floor tributary area and distributed proportionally to the floor nodes. The simulation models were calibrated to the response data measured during the Imperial Valley earthquake so as to validate and verify the analytical results of the comparative study.

Table 1 lists the linear-elastic periods of the first several modes, along with their modal participation and contribution factors (Chopra 2007) for two orthogonal directions along the

**Table 1.** Linear-Elastic Dynamic Properties of Imperial County Services Building

| Mode number ($n$) | Period ($s$) | $\Gamma_{n,x}$ | $\Gamma_{n,y}$ | MCF,x (%) | MCF,y (%) |
|---|---|---|---|---|---|
| 1 | 1.2 | 5.3 | 0.0 | 84.5 | 0.0 |
| 2 | 0.4 | 0.0 | 4.8 | 0.0 | 68.4 |
| 3 | 0.4 | −1.9 | 0.0 | 10.5 | 0.0 |
| 4 | 0.3 | 0.0 | −0.8 | 0.0 | 1.9 |
| 5 | 0.2 | −1.0 | 0.0 | 3.0 | 0.0 |
| 6 | 0.2 | −0.7 | 0.0 | 1.4 | 0.0 |

Note: The modal participation ($\Gamma$) and modal contribution factors (MCFs) are shown to illustrate how the first six modes contribute to the linear-elastic responses in two orthogonal directions.

structural axes. The fundamental mode is primarily along the moment frame (E-W direction) or X-direction of the computer model. As shown in Table 1, the period of the structure along this direction is 1.2 s, while the period of the structure in the Y-direction

**Table 2.** Selected Near-Fault Strong Ground Motion Records

| Pair number | Earthquake name | Year | Station name | $M_w$ | $R_{rup}$ (km) | $V_{S30}$ (m/s) | Fault-normal component | | | Fault-parallel component | | |
|---|---|---|---|---|---|---|---|---|---|---|---|---|
| | | | | | | | PGA (g) | PGV (cm/s) | PGD (cm) | PGA (g) | PGV (cm/s) | PGD (cm) |
| 1 | Tabas, Iran | 1978 | Tabas | 7.4 | 2.1 | 767 | 0.8 | 118 | 97 | 0.8 | 80 | 42 |
| 2 | Imperial Valley, CA | 1979 | EC Meloland Overpass FF | 6.5 | 0.1 | 186 | 0.4 | 115 | 40 | 0.3 | 27 | 15 |
| 3 | Imperial Valley, CA | 1979 | El Centro Array #7 | 6.5 | 0.6 | 211 | 0.5 | 109 | 46 | 0.3 | 45 | 24 |
| 4 | Superstition Hills, CA | 1987 | Parachute Test Site | 6.5 | 1.0 | 349 | 0.4 | 107 | 51 | 0.3 | 50 | 22 |
| 5 | Loma Prieta, CA | 1989 | Corralitos | 6.9 | 3.9 | 462 | 0.5 | 45 | 14 | 0.5 | 42 | 7 |
| 6 | Loma Prieta, CA | 1989 | LGPC | 6.9 | 3.9 | 478 | 0.9 | 97 | 63 | 0.5 | 72 | 31 |
| 7 | Erzincan, Turkey | 1992 | Erzincan | 6.7 | 4.4 | 275 | 0.5 | 95 | 32 | 0.4 | 45 | 17 |
| 8 | Northridge, CA | 1994 | Newhall—W Pico Canyon Rd | 6.7 | 5.5 | 286 | 0.4 | 88 | 55 | 0.3 | 75 | 22 |
| 9 | Northridge, CA | 1994 | Rinaldi Receiving Sta | 6.7 | 6.5 | 282 | 0.9 | 167 | 29 | 0.4 | 63 | 21 |
| 10 | Northridge, CA | 1994 | Sylmar—Converter Sta | 6.7 | 5.4 | 251 | 0.6 | 130 | 54 | 0.8 | 93 | 53 |
| 11 | Northridge, CA | 1994 | Sylmar—Converter Sta East | 6.7 | 5.2 | 371 | 0.8 | 117 | 39 | 0.5 | 78 | 29 |
| 12 | Northridge, CA | 1994 | Sylmar—Olive View Med FF | 6.7 | 5.3 | 441 | 0.7 | 123 | 32 | 0.6 | 54 | 11 |
| 13 | Kobe, Japan | 1995 | Takatori | 6.9 | 1.5 | 256 | 0.7 | 170 | 45 | 0.6 | 63 | 23 |
| 14 | Kocaeli, Turkey | 1999 | Yarimca | 7.4 | 4.8 | 297 | 0.3 | 48 | 43 | 0.3 | 73 | 56 |
| 15 | Chi-Chi, Taiwan | 1999 | TCU052 | 7.6 | 0.7 | 579 | 0.4 | 169 | 215 | 0.4 | 110 | 220 |
| 16 | Chi-Chi, Taiwan | 1999 | TCU065 | 7.6 | 0.6 | 306 | 0.8 | 128 | 93 | 0.6 | 80 | 58 |
| 17 | Chi-Chi, Taiwan | 1999 | TCU068 | 7.6 | 0.3 | 487 | 0.6 | 191 | 371 | 0.4 | 238 | 387 |
| 18 | Chi-Chi, Taiwan | 1999 | TCU084 | 7.6 | 11.2 | 553 | 1.2 | 115 | 32 | 0.4 | 44 | 21 |
| 19 | Chi-Chi, Taiwan | 1999 | TCU102 | 7.6 | 1.5 | 714 | 0.3 | 107 | 88 | 0.2 | 78 | 55 |
| 20 | Duzce, Turkey | 1999 | Duzce | 7.2 | 6.6 | 276 | 0.4 | 62 | 47 | 0.5 | 80 | 48 |

Note: $M_w$ = moment magnitude; PGA = peak ground acceleration; PGV = peak ground velocity; PGD = peak ground displacement; $R_{rup}$ = closest distance to co-seismic rupture plane; $V_{S30}$ = average shear-wave velocity of upper 30 m of site.

is 0.4 s, which is the period of the second mode. The irregularities in the N-S stiffness at the ground floor appear to have resulted in excessive torsional response and in significant coupling of the N-S and torsional excitations and responses. For the N-S (or Y) direction, the structure is not first-mode dominated because the modal contribution factor for the first mode in this direction is only 68%.

## Ground Motions Selected

For this investigation, 20 near-fault strong motion records, listed in Table 2, were selected from 10 shallow crustal earthquakes compatible with the following scenario:
- Moment magnitude: $M_w = 6.7 \pm 0.2$
- Closest-fault distance: $0.1 \le R_{rup} \le 11$ km
- NEHRP soil type: C or D

Shown in Fig. 3 are the 5% damped response spectra for the X- and Y-components of the as-recorded ground motions. Also shown is the median spectrum, computed as the geometric mean of 20 response spectra in each direction. The median spectra show significantly large demands at the first and second modes of the building in both directions.

## Methodology for Evaluation of Fault-Normal/Parallel Directions

Restricting ourselves to the linear-elastic version of the structural model, we invoke the principle of superposition (to be elaborated as follows) to compute structural responses for a large number of seismic rotation angles. When subjected to a single horizontal component of ground motion, the equation of motion for a 2D multistory building is (Chopra 2007)

$$\mathbf{m}\ddot{u} + \mathbf{c}\dot{u} + \mathbf{k}u = \mathbf{P}_{eff} = -\mathbf{m}i\ddot{u}_g \quad (1)$$
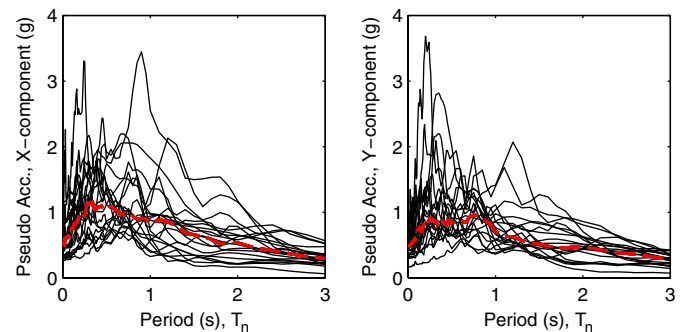


**Fig. 3.** Pseudo-acceleration response spectra of 20 near-fault strong ground motions; damping ratio 5% (dashed line = median spectrum of all records)

where $\mathbf{m}$, $\mathbf{c}$, and $\mathbf{k} = N \times N$ square matrices (where $N$ is the number of dynamic DOFs) that define the structural properties of the building. In this case, the effective earthquake force $\mathbf{P}_{eff}$ consists of a single horizontal component of ground motion $\ddot{u}_g$ applied along the direction specified by the influence vector $i$. However, when analyzing a 3D multistory building, subjected to two horizontal components of ground motion, one must include a larger number of DOFs in the structural matrices and appropriately modify the effective earthquake force (Goel and Chopra 2004; Athanatopoulou 2005). If one applies the two as-recorded horizontal components of ground motion, denoted as $\ddot{u}_{gx}$ and $\ddot{u}_{gy}$, directly along the structural axes, then the effective earthquake force becomes

$$\mathbf{P}_{eff} = -\mathbf{M}(i_x\ddot{u}_{gx} + i_y\ddot{u}_{gy}) \quad (2)$$

where the influence vectors $i_x$ and $i_y$ refer to the displacement of the lumped masses when the structure is subjected to a unit ground displacement along the $X$ and $Y$ structural axes, respectively. To obtain the structural responses when the building is subjected to a horizontally rotated version of the as-recorded ground motion

pair, denoted as $\ddot{u}_{gx}^{(arb)}$ and $\ddot{u}_{gy}^{(arb)}$, we modify the effective earthquake force as

$$
\begin{aligned}
\mathbf{P}_{eff}^{(arb)} &= -\mathbf{M}(i_x \ddot{u}_{gx}^{(arb)} + i_y \ddot{u}_{gy}^{(arb)}) \\
&= -\mathbf{M}[i_x(\cos\theta \ddot{u}_{gx} - \sin\theta \ddot{u}_{gy}) + i_y(\sin\theta \ddot{u}_{gx} + \cos\theta \ddot{u}_{gyy})] \\
&= -\mathbf{M}(\cos\theta(i_x \ddot{u}_{gx} + i_y \ddot{u}_{gy}) + \sin\theta[i_x(-\ddot{u}_{gy}) + i_y \ddot{u}_{gx}]\} \\
&= \cos\theta[-\mathbf{M}(i_x \ddot{u}_{gx} + i_y \ddot{u}_{gy})] + \sin\theta\{-\mathbf{M}[i_x(-\ddot{u}_{gy}) + i_y \ddot{u}_{gx}]\} \\
&= \cos\theta(\mathbf{P}_{eff}^{(1)}) + \sin\theta(\mathbf{P}_{eff}^{(2)})
\end{aligned}
\tag{3}
$$

where $\theta$ = an arbitrary seismic rotation angle of interest. Eq. (3) shows that $\mathbf{P}_{eff}^{(arb)}$ is a linear combination of two excitations; $\mathbf{P}_{eff}^{(1)}$ corresponds to the excitation where the as-recorded ground motion pair is applied directly to the structural axes, whereas $\mathbf{P}_{eff}^{(2)}$ corresponds to the excitation where the as-recorded ground motion pair is first rotated 90° clockwise before being applied to the structural axes. Using the principle of superposition for a fixed response quantity of interest, the response history for any arbitrary seismic rotation angle $r^{(arb)}$ may be computed as a linear combination of two response histories—one corresponding to $\mathbf{P}_{eff}^{(1)}$ and the other corresponding to $\mathbf{P}_{eff}^{(2)}$:

$$
r^{(arb)} = \cos\theta r^{(1)} + \sin\theta r^{(2)}
\tag{4}
$$

where $r^{(1)}$ = response history under excitation $\mathbf{P}_{eff}^{(1)}$; and $r^{(2)}$ = response history under excitation $\mathbf{P}_{eff}^{(2)}$.

Viewing the response as both a function of time and rotation angle enables us to better understand how the critical angle $\theta_{cr}$, defined as the angle corresponding to the largest response over all nonredundant rotation angles, varies with both EDP and ground motion pair. For a given response quantity of interest and record pair, the FN/FP directions will correspond to two values (i.e., FN and FP rotated ground motions are applied along the $X$- and $Y$-axes, then along the $Y$- and $X$-axes of the structure). By comparing these two values with the structural responses at all other possible angles, one can evaluate the level of conservatism in such directions. If obvious systematic benefits of the FN/FP orientations existed, they should be observable by repeating such comparisons for several EDPs and record pairs.

Even if no obvious trends are observed, one can still compare the FN/FP directions with the no rotation case. Rather than comparing the FN/FP directions to the as-recorded directions, however, the as-recorded direction may be viewed as an arbitrarily assigned orientation. As a result, one will be able to state the likelihood of the
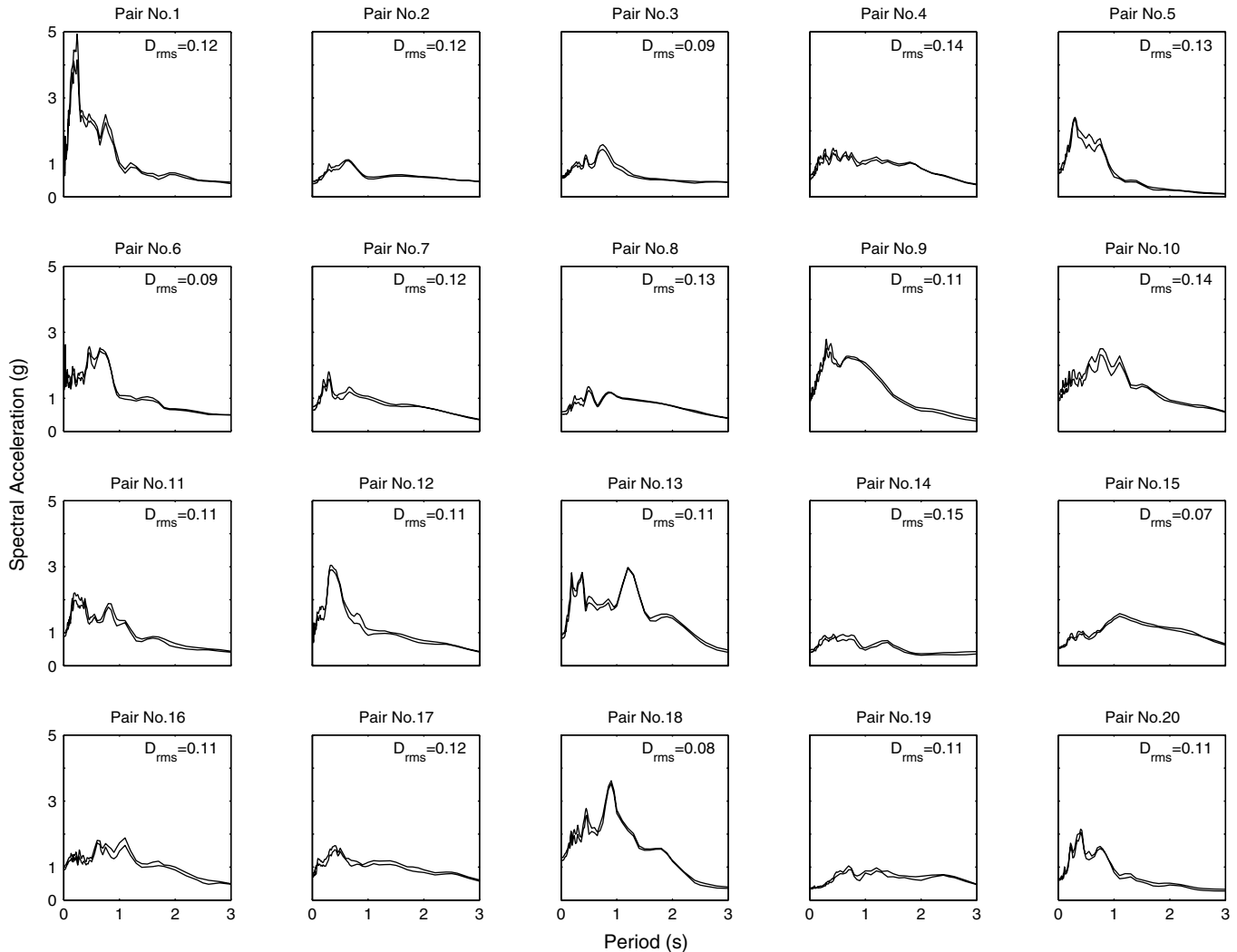


**Fig. 4.** Maximum and minimum envelopes for square-root-of-sum-of-squares (SRSS) response spectra rotated through all angles from 0 through 180° with 5° interval; root-mean-square ($D_{rms}$) metric is shown for each horizontal pair of ground motion to indicate degree of variation in rotated spectra; small values of $D_{rms}$ in all panels indicate that variation of spectral values by rotating ground motion components is insignificant

FN/FP responses being conservative instead of simply stating whether or not it was conservative.

If the rotation angle $\theta$ for a record pair was the only source of uncertainty and the probability distribution for $\theta$ was specified, then a conditional probability density function (PDF) for the structural response may be defined. In particular, if $\theta$ is uniformly distributed from 0 through 180°, then the PDF for the EDP may be estimated by (1) obtaining a random sample of $n$ rotation angles based on the uniform distribution, (2) computing the EDP corresponding to each of the $n$ angles, and (3) forming a histogram with the collection of EDP values (Wasserman 2004). Equipped with an estimate of the EDP's probability distribution, conditioned on a ground motion pair, one can approximately determine the probability of exceeding the FN/FP responses. Low probabilities of exceedance would suggest that there is some merit in focusing our attention on the FN/FP directions.

## Structural Response Variability with Rotation Angle

According to the ASCE/SEI-7 provisions under Section 16.1.3.2, the horizontal components are to be identically scaled such that the average of the SRSS spectra from all scaled horizontal component pairs exceeds the target design spectrum (defined under ASCE/SEI-7, Section 11.4.5 or 11.4.7) over the period range of $0.2T_1$ to $1.5T_1$.

### How Will the SRSS Spectrum Change if the Ground Motion Pair is Rotated?

By rotating each of the 20 record pairs in Table 2 from 0 to 180° with a 5° interval in the clockwise direction, one can compute 37 alternative SRSS spectra. Fig. 4 shows the maximum and minimum envelopes bounding such rotated versions of the SRSS response spectra for each ground motion pairs (no scaling is applied). In this figure, $D_{rms}$ refers to root mean square, a metric used to quantify the variability of spectral accelerations (Sa) with changing rotation angle. $D_{rms}$ is computed for each rotation angle over all spectral periods as

$$D_{rms} = \sqrt{\frac{1}{N}\sum_{i=1}^{N}[\ln(Sa_{max,i}) - \ln(Sa_{min,i})]^2} \qquad (5)$$

where $i$ refers to the $i$th spectral period and $N$ is the total number of logarithmically spaced spectral periods. It is visually evident that
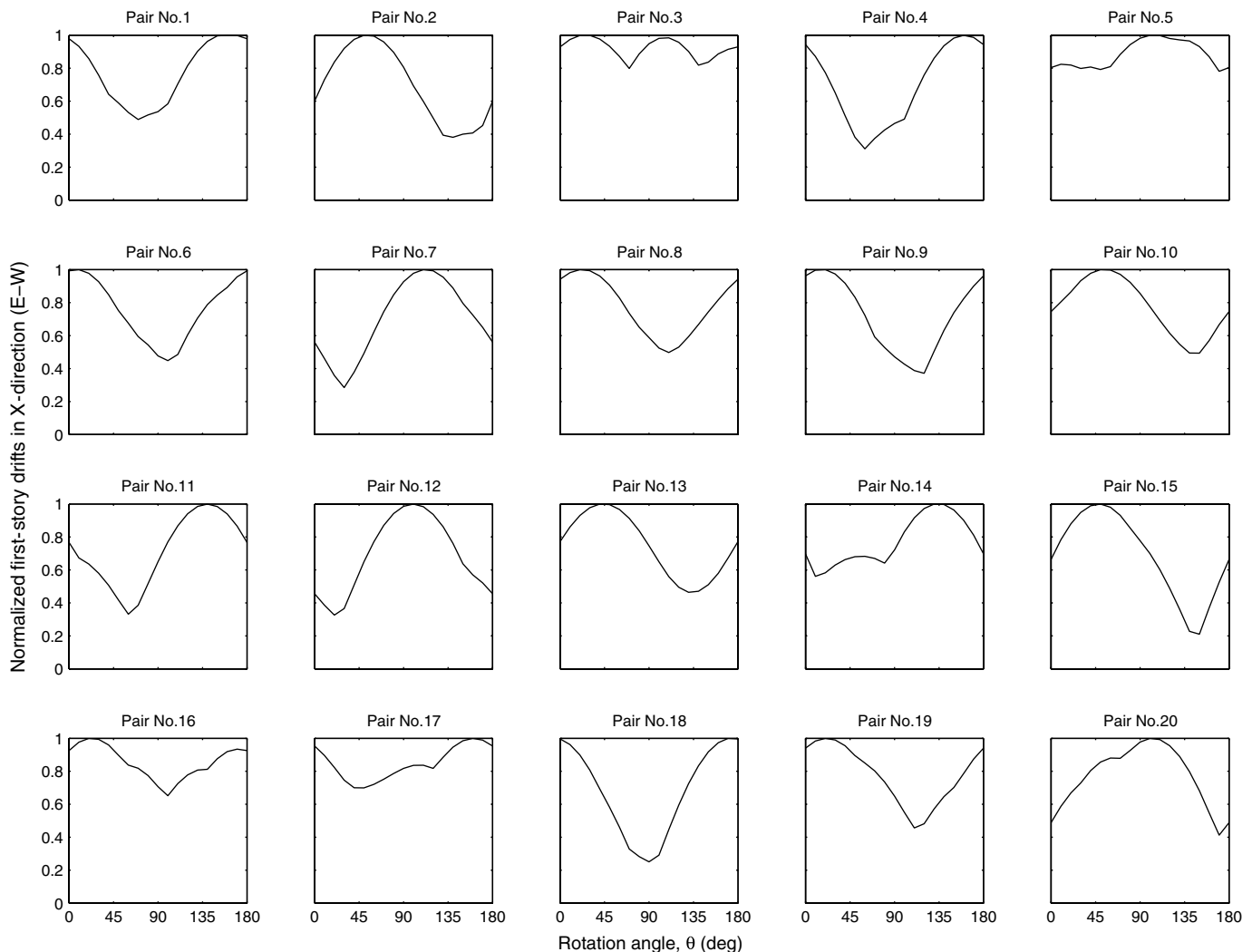


**Fig. 5.** Normalized first-story drift in longitudinal direction (X or east-west) as a function of clockwise rotation angle $\theta$ for 20 ground motion pairs; the normalizing factor is the maximum value over all angles for the ground motion pair being considered; this factor differs for each pair; this figure shows that story drift can vary by a factor of 2 over the possible angles of interest. (Note: FN direction is not necessarily at 0°)

the SRSS response spectrum vary marginally with rotation angle. The relatively small $D_{rms}$ values indicate that several rotated versions of the ground motion pair can satisfy the ASCE criteria and yet provide structural responses that are different (as shown later). This figure also implies that rotating ground motions have a marginal effect on the ground motion scaling factors computed for each pair to satisfy the ASCE criteria.

### How Much Variability is there in the Elastic Structural Responses as the Rotation Angle is Varied?

Fig. 5 addresses this question by showing the drifts in the longitudinal (E-W or X) direction for the first story as a function of

the rotation angle for all records. To better understand the relative variability, each subplot was normalized by the maximum response over all angles. Maximum responses for individual ground motion pairs were found to occur at different angles. With the exception of a few pairs, the first-story drift (i.e., interstory drift) in the X-direction can vary by a factor of 2 over the possible angles of interest. This is considered to be a large variation.

Although this figure indicates that the first-story drift in the X-direction does not vary significantly with rotation angle for ground motion Pair No. 3, the same statement cannot be made for other response quantities. Considering Pair No. 3, various other response quantities are shown as a function of rotation angle in Fig. 6. It is evident that peak values of other EDPs occur at different
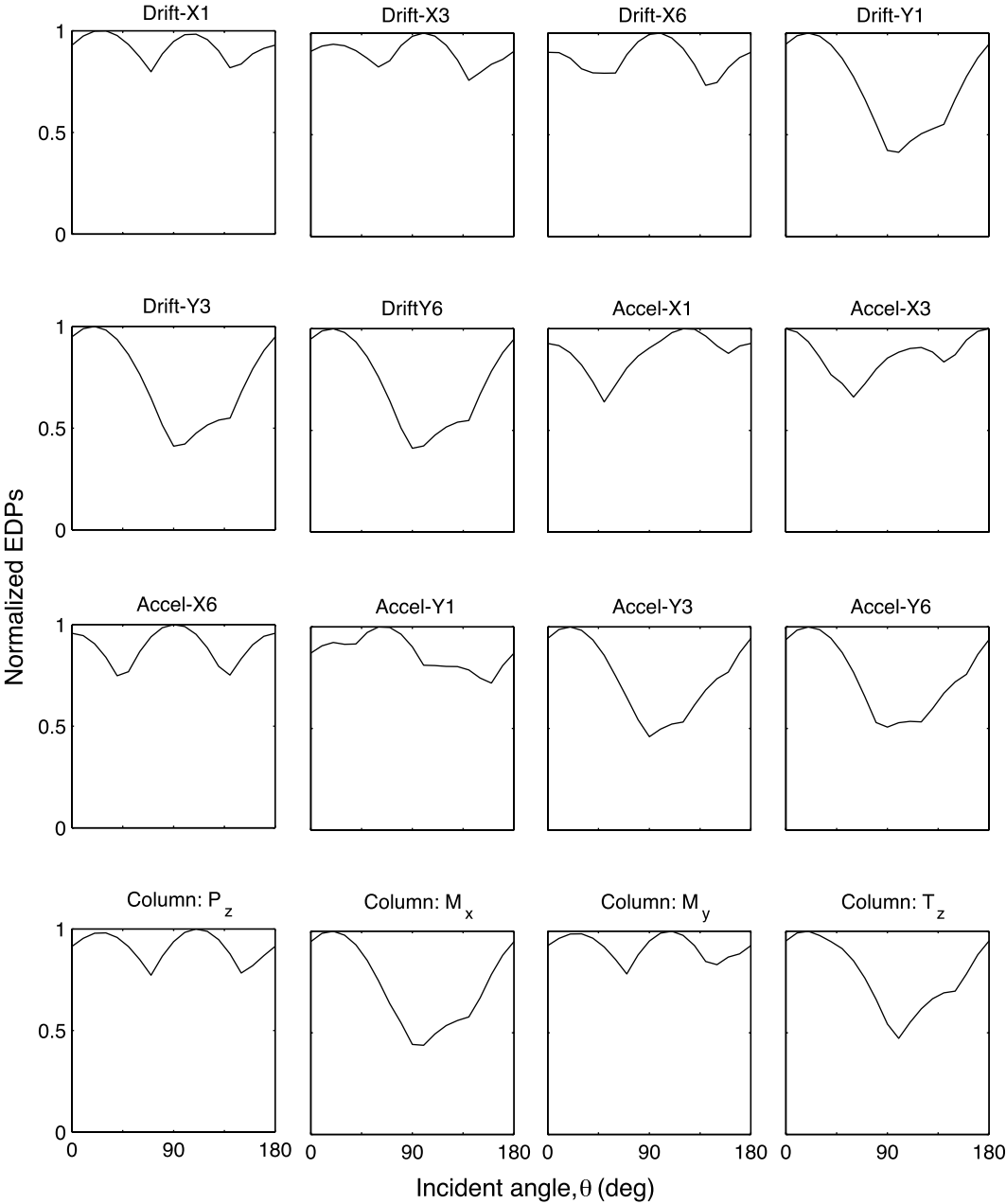


**Fig. 6.** For ground motion Pair No. 3, normalized engineering demand parameters (EDPs) show different degree of variation with respect to clockwise rotation angle $\theta$. In this figure, $P_z$, $M_x$, $M_y$, and $T_z$ correspond to the first-story corner column's axial force, moments about two orthogonal directions, and torsion; the number following the X- or Y-direction indicates the floor, for example, Accel-X6 means sixth floor acceleration along X-direction. (Note: FN direction is not necessarily at 0°)

**Table 3.** Coefficient of Variation for Force (P) and Moment (M or T) Parameters along X-, Y-, and Z-Directions of a First-Story Corner Column

| Pair number | Coefficient of variation for arbitrary first-story corner column | | | | | |
|---|---|---|---|---|---|---|
| | $P_x$ (kips) | $P_y$ (kips) | $P_z$ (kips) | $M_x$ (kip-in) | $M_y$ (kip-in) | $T_z$ (kip-in) |
| 1 | 0.26 | 0.29 | 0.28 | 0.29 | 0.26 | 0.23 |
| 2 | 0.36 | 0.15 | 0.12 | 0.17 | 0.35 | 0.21 |
| 3 | 0.08 | 0.27 | 0.14 | 0.28 | 0.07 | 0.22 |
| 4 | 0.34 | 0.16 | 0.17 | 0.17 | 0.36 | 0.16 |
| 5 | 0.09 | 0.34 | 0.26 | 0.36 | 0.05 | 0.32 |
| 6 | 0.17 | 0.25 | 0.21 | 0.27 | 0.24 | 0.23 |
| 7 | 0.35 | 0.09 | 0.12 | 0.07 | 0.34 | 0.14 |
| 8 | 0.24 | 0.12 | 0.09 | 0.14 | 0.22 | 0.09 |
| 9 | 0.29 | 0.16 | 0.07 | 0.18 | 0.29 | 0.21 |
| 10 | 0.24 | 0.14 | 0.09 | 0.17 | 0.23 | 0.18 |
| 11 | 0.30 | 0.24 | 0.22 | 0.26 | 0.31 | 0.26 |
| 12 | 0.22 | 0.39 | 0.32 | 0.39 | 0.30 | 0.37 |
| 13 | 0.28 | 0.07 | 0.20 | 0.08 | 0.25 | 0.10 |
| 14 | 0.20 | 0.17 | 0.14 | 0.16 | 0.20 | 0.10 |
| 15 | 0.41 | 0.28 | 0.09 | 0.26 | 0.38 | 0.27 |
| 16 | 0.12 | 0.07 | 0.15 | 0.06 | 0.12 | 0.06 |
| 17 | 0.11 | 0.26 | 0.22 | 0.27 | 0.12 | 0.27 |
| 18 | 0.40 | 0.27 | 0.13 | 0.27 | 0.39 | 0.27 |
| 19 | 0.24 | 0.21 | 0.12 | 0.21 | 0.23 | 0.19 |
| 20 | 0.25 | 0.28 | 0.22 | 0.27 | 0.25 | 0.18 |

Note: X = longitudinal; Y = transverse; Z = vertical direction in plan view.

angles for the same record pair. Large variation for EDPs other than story drift is also observed. For example, the torsion for an arbitrarily selected column can vary by a factor of 2 over the possible angles.

To better quantify this variation with rotation angle, the coefficient of variation (COV) is computed using Eq. (6) for each ground motion pair and for each response quantity related to an arbitrarily selected corner column in the first story (these values are shown in Table 3):

$$\mathrm{COV} = \frac{\sqrt{\frac{1}{n-1} \sum_{n-1}^{n} (x_i - \bar{x})^2}}{\bar{x}} \qquad (6)$$

The COV for $M_x$ is larger for Pair No. 1 than for Pair No. 2. The reverse is true, however, when the response quantity of interest is $M_y$ instead. Here, the COV is larger for the second pair than for the first pair. These results demonstrate that one must consider both the response quantity of interest and the ground motion characteristics when attempting to predict the variability with respect to rotation angle in advance.

The fact that the variability depends on both the response quantity and ground motion pair can also be observed in Fig. 7, where the heightwise distribution of story drifts in the X-direction over several angles is shown. To illustrate the variability in the responses within each pair, a common scale was not used for the drift axis.
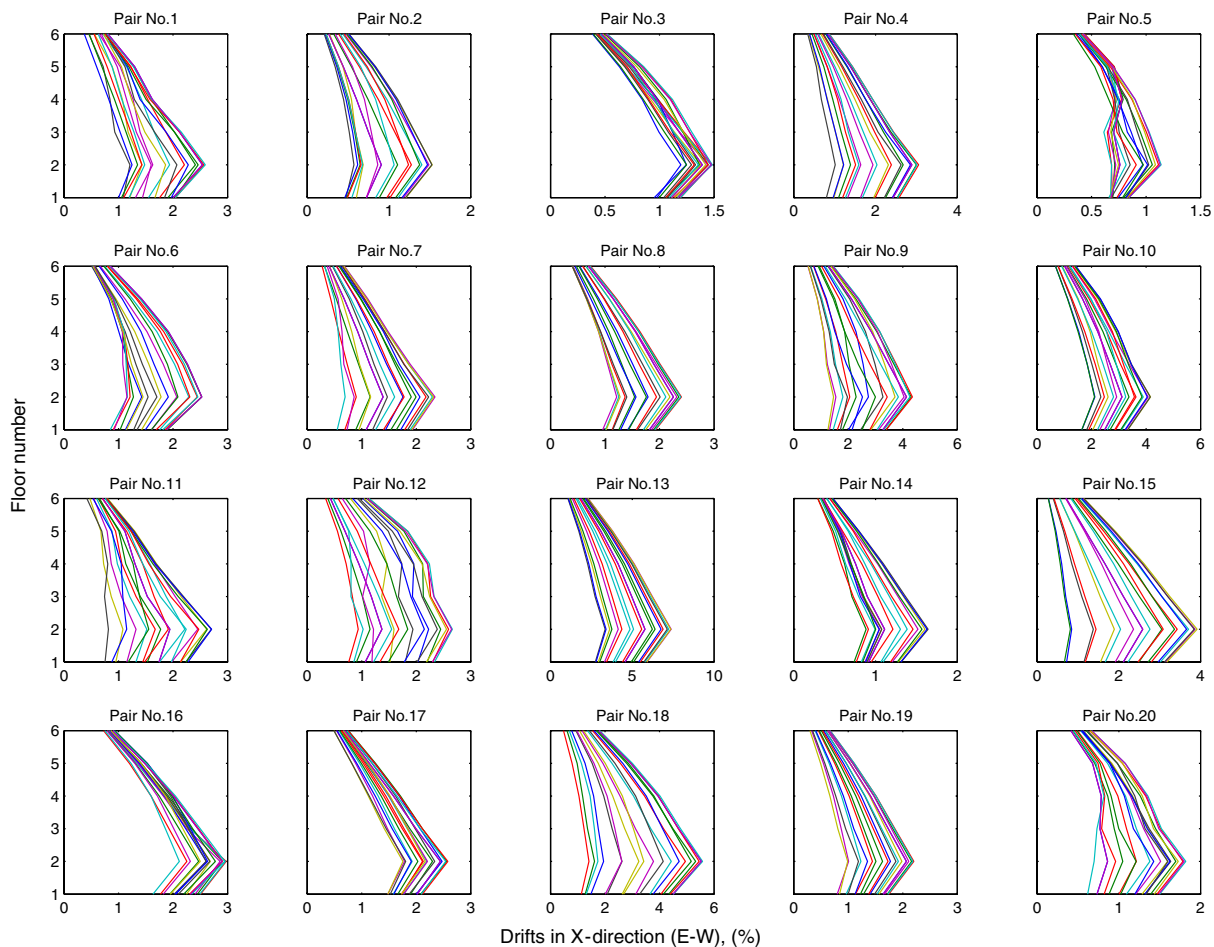


**Fig. 7.** Story drift profiles in longitudinal (X or east-west) direction for 20 ground motion pairs rotated 0 through 180° clockwise with an interval of 10°. To illustrate the relative variability with respect to the rotation angle, a common scale was not used
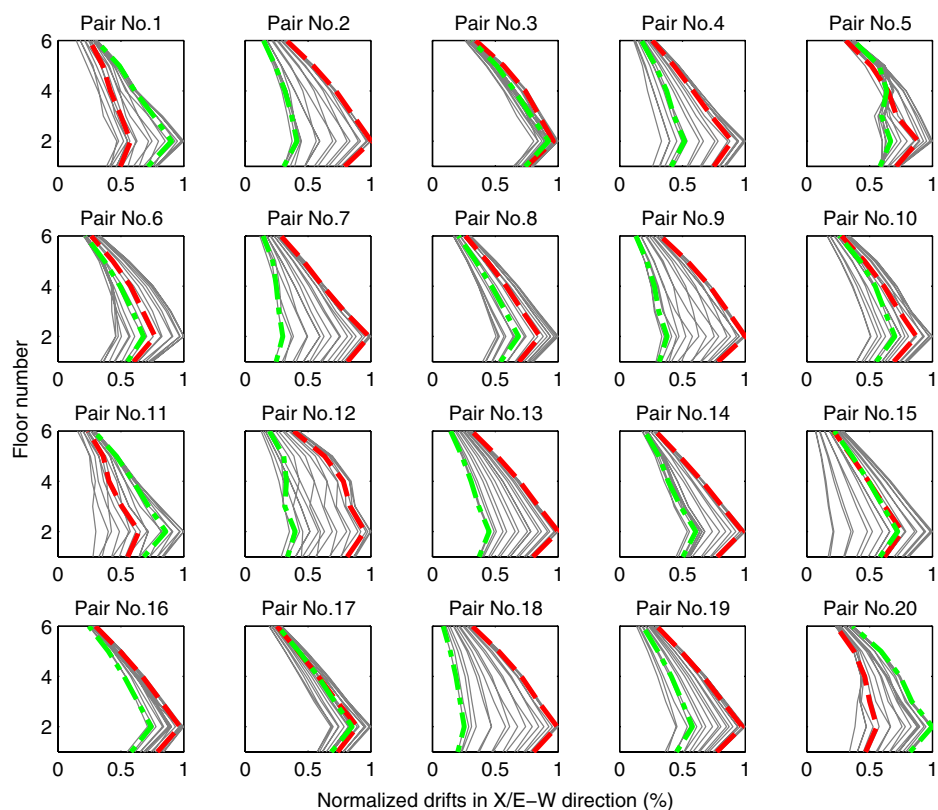
**Fig. 8.** Story drift profiles in longitudinal (X or east-west) direction; angles corresponding to fault-normal and fault-parallel directions shown by dashed and dashed-dotted lines, respectively
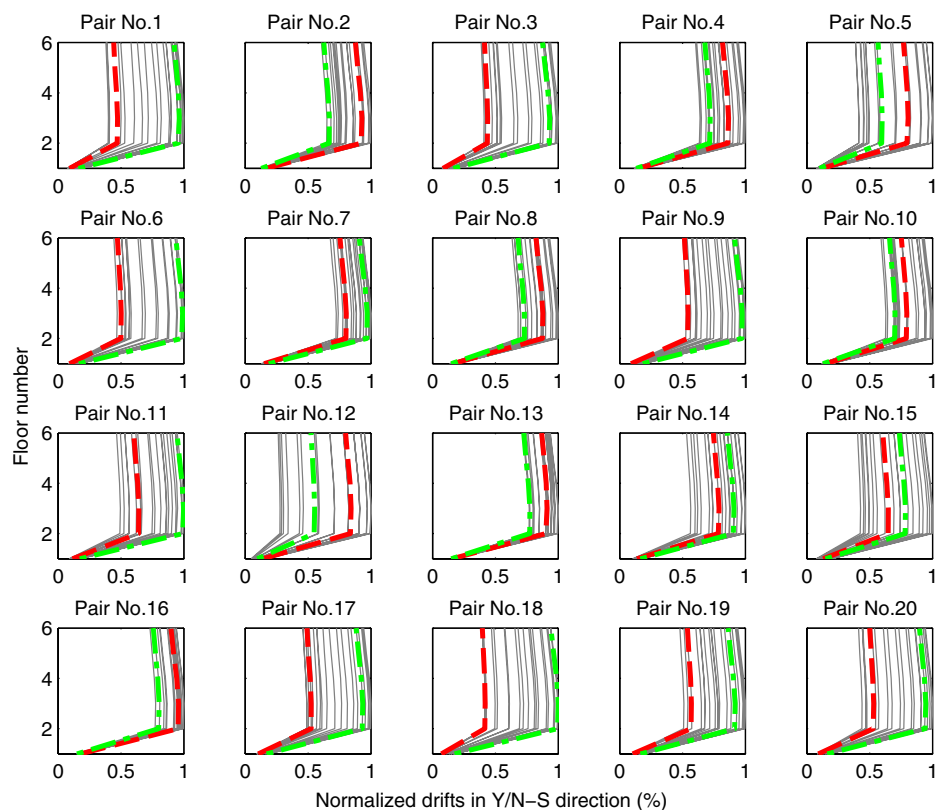


**Fig. 9.** Story drift profiles in transverse (Y or north-south) direction; angles corresponding to fault-normal and fault-parallel directions shown by dashed and dashed-dotted lines, respectively

The variability was significantly large for some ground motion pairs (e.g., Pair Nos. 12, 15, and 18), as compared to smaller variability observed for Pair Nos. 3, 16, and 17. For the fifth pair of ground motion, the larger drift in the fourth story indicates higher-mode effects. Contribution of higher-mode effects to the response with larger demands at upper stories becomes more pronounced at certain angles only. Similar results for the Y-direction are shown in Kalkan and Kwong (2012). These results also confirm the fact that $\theta_{cr}$ varies with ground motion and with response quantity of interest. This is because $\theta_{cr}$ is a quantity that is highly dependent on the complete response history of the EDP. As a result, determining a rotation angle that yields a conservative estimate of structural response simultaneously for both a large number of response quantities (EDPs) and ground motion records is difficult; it is easy, however, to compute $\theta_{cr}$ for a single EDP under a single pair of accelerograms (Athanatopoulou 2005).

## Evaluation of Fault-Normal/Parallel Direction Rotated Ground Motion

To evaluate the usefulness of rotating a record pair in the FN/FP directions, a practice commonly used, the EDPs corresponding to the FN/FP directions are compared against those corresponding to all other directions. To limit the computations to a reasonable size, each as-recorded pair is rotated clockwise by increments of 10° instead of 5° before the EDPs are calculated. As a result, the two FN/FP sets of responses are compared against 19 other sets.

For example, the 21 heightwise distributions of story drifts in the X-direction, for each record pair, are shown in Fig. 8; plots showing drifts in the Y-direction are shown in Kalkan and Kwong (2012). The distribution of drifts corresponding to the FN direction is highlighted in red, while that corresponding to the FP direction is highlighted in green. To display the variability in responses within each pair, the drift values are normalized by the maximum drift value over all 19 angles and over the entire height. For some pairs (e.g., Pair Nos. 5, 6, and 8), the maximum of the FN/FP drifts is not the largest among all possibilities. Visually, the maximum of the FN/FP drifts is the largest among all possibilities approximately only for 10 of the 20 record pairs. Consequently, the FN/FP drifts are not always conservative.

Whether or not the FN/FP drifts are conservative depends not only on the ground motion pair but also on the EDP. For instance, although the FN direction yields the maximum heightwise distribution of drifts in the X-direction for Pair No. 18, the FN direction yields the minimum heightwise distribution of drifts in the
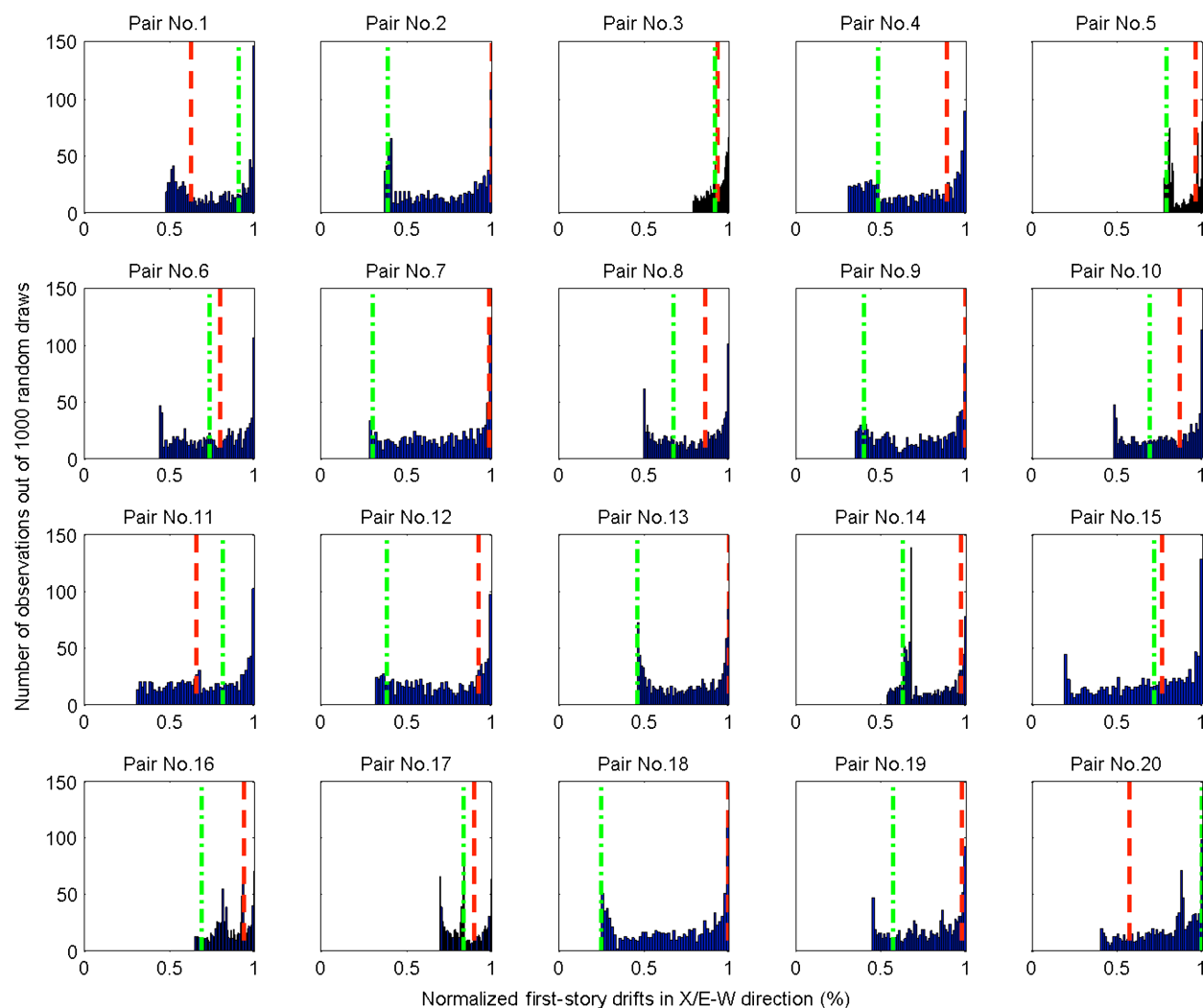


**Fig. 10.** Histogram of 1,000 randomly obtained realizations of first-story drift in X-direction; dashed line = value corresponding to fault-normal direction; dashed-dotted line = value corresponding to fault-parallel direction

Y-direction for the same pair, as demonstrated in Fig. 9. As another example, although the FP direction yields the largest roof drift in the X-direction for Pair No. 5, the same direction for the same pair does not guarantee a conservative first-story drift in the X-direction, as demonstrated in Fig. 8. Thus, one cannot be certain that the worst-case responses are always obtained when performing RHAs with ground motions rotated to the FN/FP directions.

### If the FN/FP Directions Do Not Generate the Maximum Responses for All Response Quantities and for All Ground Motion Pairs, is there Still an Advantage to Rotating an as-recorded Pair Prior to Performing Response History Analyses?

To address this issue, the FN/FP direction rotated ground motions are evaluated from a statistical viewpoint. Suppose the only source of aleatoric uncertainty in responses is due to uncertainty in the rotation angle of the ground motion pair. In other words, given the structural model and ground motion pair, the EDP will have a probability distribution that is directly related to the probability distribution for the rotation angle. This conditional distribution for the EDP can serve as a benchmark to evaluate the usefulness in rotating as-recorded ground motions to the FN/FP directions.

Because the functional relationship between the EDP and the rotation angle is different for each EDP of interest, the conditional probability distribution will be different for different EDPs. Moreover, because the functional relationship is generally complex (especially for nonlinear-inelastic systems), direct analytical determination of the probability distribution is not feasible. Consequently, Monte Carlo simulation is used here to estimate these distributions. Assuming the rotation angle is a uniformly distributed random variable, a random sample of angles is generated. For each angle in the random sample, the EDP of interest is determined. Summarizing such data in the form of histograms, for all record pairs and for the first story drift in the X-direction, leads to the plots shown in Fig. 10; similar plots for the Y-direction are shown in Kalkan and Kwong (2012).

The histograms in this figure may be interpreted as approximate PDFs for the normalized EDPs (normalized by their maximum values). The normalized scales confirm that the response variability depends on both the record pair and the EDP of interest. These approximate densities are bounded since the range of possible rotation angles is finite. A majority of the approximate PDFs share a common shape. Specifically, the distributions appear to be bimodal, with the modal values often at the extremes, also valid for other EDPs. A rough interpretation of this is that if one were to determine
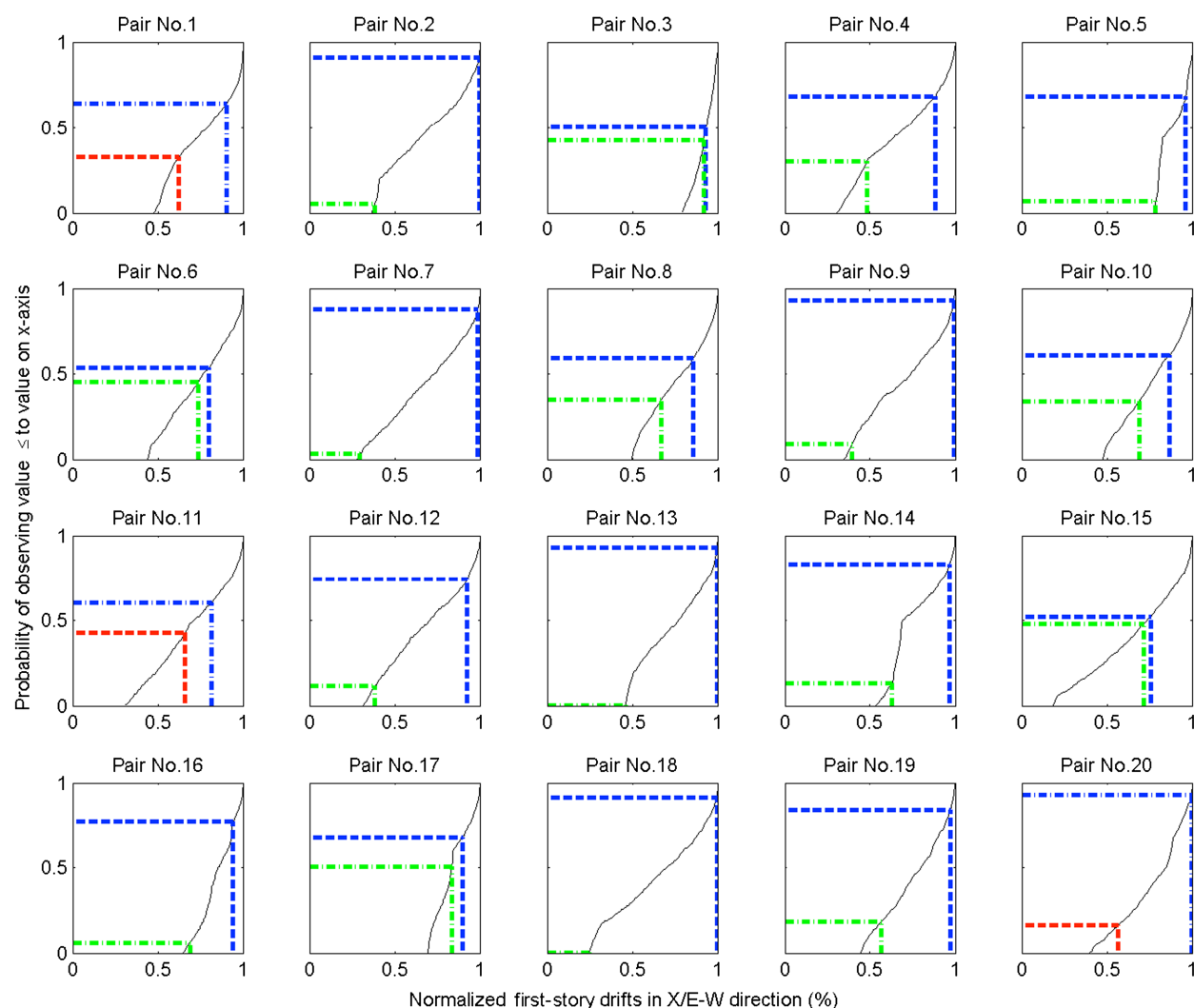


**Fig. 11.** For a given pair of ground motion and a given value of first-story drifts in X-direction, the probability of observing an engineering demand parameter (EDP) value equal to or less than the given EDP value is shown based on 1,000 realizations; red line = EDP value corresponding to fault-normal direction; green line = EDP value corresponding to fault-parallel direction; blue line = larger of FN/FP responses

---

© ASCE

04013062-11

J. Struct. Eng.

the EDP corresponding to a randomly chosen angle, the EDP would most likely be a maximum or a minimum value (rather than somewhere in between) with respect to all possible values. If one were to take the EDP as the larger of the FN/FP EDPs instead, Fig. 10 illustrates that the value would usually be larger than half of all possible responses.

To quantify the latter observations, the concept of cumulative distribution functions [CDFs; the CDF of $x$, or $F(x)$, indicates the probability of observing a value equal to or less than the value of $x$] is utilized. Approximate CDFs for the normalized first story drifts in the X-direction are shown in Fig. 11 [similar plots are shown for the Y-direction in Kalkan and Kwong (2012)]. This figure is simply the data from Fig. 10 replotted in a different way. The steep slope near the ends of the CDFs is consistent with the previous observation that responses near the extremes of the possible range have higher probabilities of occurring relative to other values. To understand what information the larger (blue) of the FN (red) and FP (green) responses provide, we will focus on the first subplot in Fig. 11. The subplot indicates that there is approximately a 65% probability of observing a first-story-drift value less than or equal to the FP value identified in blue (in this case it is also the larger of the FN/FP values). Equivalently, there is approximately a 35% probability that the FP value will underestimate the drift for precisely record Pair No. 1. Focusing on the blue lines for all record pairs next, one observes that the probability of observing a drift value larger than the maximum of the FN/FP value is consistently less than 50% for all record pairs. However, this trend is not perfect, as demonstrated for Pair Nos. 8 and 13 for the Y-direction drifts in Kalkan and Kwong (2012).

The CDFs, and the associated probability statements, are approximate because the empirical cumulative distribution functions (ECDFs) were shown instead of the true CDFs. In probability and statistics, the ECDF is an estimate of the CDF obtained using a random sample from the true CDF (Wasserman 2004). Assigning an equal probability to each value in the random sample of size $n$ and using Eq. (7) leads to a staircase curve known as the ECDF:

$$\hat{F}_n(t) = \frac{1}{n} \sum_{i=1}^{n} 1\{X_i \le t\} \qquad (7)$$

where $X_i = i$th value in the random sample of size $n$; and $1$ = indicator function—it is 1 only if the event in the brackets is true and 0 otherwise. As the sample size increases, the ECDF converges almost surely to the true CDF because of the Glivenko-Cantelli theorem (Dudley 1999). This is shown in Kalkan and Kwong (2012) when 100, 1,000, and 5,000 different random samples of the first-story drift in the X-direction are used to compute the ECDF. The curve corresponding to the use of 1,000 values is virtually indistinguishable from that associated with the use of 5,000 values. As a result, 1,000 values were used to construct the histograms and ECDFs in the previous figure.

Since the conditional ECDFs vary depending on response quantity, the benchmark evaluations of the FN/FP directions should be performed considering several response quantities. Using a sample size of 5,000, Table 4 shows the probabilities of exceeding the larger of the FN/FP responses for story drifts in all stories and in both orthogonal directions of the structure. These probabilities of exceedance may be interpreted as the amount of error one makes in deciding to use the larger of the FN/FP response as the worst-case value among all possibilities. Considering errors from round-off and the use of a finite random sample, Table 4 numerically confirms that there is always some probability of obtaining a response value larger than that associated with the FN and FP directions. In other words, there is always some amount of error made when deciding to use the FN/FP response as the worst among all angles. However, the cells with probabilities smaller than 15% (indicated by bold font) may be viewed as instances where the FN/FP value is essentially conservative (15% is a widely accepted threshold for safety for engineering applications). It is numerically confirmed in Table 4 that such conservatism typically varies with response quantities and record pair.

With such numerical results one can address whether rotation in the FN/FP directions is worthwhile. One alternative to deliberate

**Table 4.** Probabilities of Exceeding Larger Response among FN/FP Values for Selected Response Quantities, Estimated with 5,000 Random Samples

| Pair number | Probability of exceeding larger response among FN/FP responses (%) | | | | | | | | | | | |
|---|---|---|---|---|---|---|---|---|---|---|---|---|
| | $DR_{x,1}$ | $DR_{x,2}$ | $DR_{x,3}$ | $DR_{x,4}$ | $DR_{x,5}$ | $DR_{x,6}$ | $DR_{y,1}$ | $DR_{y,2}$ | $DR_{y,3}$ | $DR_{y,4}$ | $DR_{y,5}$ | $DR_{y,6}$ |
| 1 | 35 | 28 | 26 | 19 | **14** | 15 | 30 | 25 | 24 | 24 | 23 | 23 |
| 2 | **0** | **1** | **4** | **7** | **9** | **10** | 28 | 25 | 25 | 25 | 25 | 25 |
| 3 | 49 | 38 | **15** | **13** | **12** | **11** | 26 | 25 | 25 | 25 | 25 | 25 |
| 4 | 30 | 30 | 27 | 25 | 26 | 27 | 42 | 38 | 38 | 38 | 38 | 38 |
| 5 | 32 | 38 | 42 | *65* | *58* | 35 | 44 | 40 | 40 | 40 | 40 | 40 |
| 6 | 46 | 46 | 46 | 45 | 44 | 43 | **13** | **10** | **9** | **9** | **9** | **9** |
| 7 | **11** | **12** | **14** | 15 | **15** | 15 | 17 | 25 | 25 | 26 | 26 | 26 |
| 8 | 40 | 41 | 41 | 40 | 39 | 39 | *57* | 46 | 45 | 45 | 44 | 44 |
| 9 | **0** | **3** | **7** | **11** | **14** | **14** | **12** | 16 | 16 | 17 | 17 | 17 |
| 10 | 38 | 38 | 41 | 44 | 46 | 46 | 45 | 46 | 46 | 46 | 46 | 46 |
| 11 | 40 | 35 | 31 | 27 | 20 | 28 | **6** | **5** | **5** | **5** | **5** | **5** |
| 12 | 25 | 21 | 20 | 25 | 28 | 29 | 39 | 38 | 38 | 38 | 38 | 38 |
| 13 | **4** | **4** | **3** | **3** | **3** | **4** | 72 | *61* | *60* | *56* | *55* | *54* |
| 14 | 15 | **14** | **12** | **12** | **14** | 16 | 30 | 33 | 33 | 33 | 33 | 33 |
| 15 | 47 | 48 | 49 | *50* | 49 | 49 | 46 | 44 | 44 | 44 | 44 | 44 |
| 16 | 23 | 31 | **15** | **15** | 30 | 31 | 20 | 45 | 45 | 46 | 47 | 46 |
| 17 | 32 | 34 | 37 | 47 | 49 | 48 | 26 | 24 | 24 | 24 | 24 | 24 |
| 18 | **7** | **8** | **11** | **12** | **13** | **13** | **5** | **4** | **4** | **4** | **4** | **4** |
| 19 | **15** | 15 | 17 | 18 | 19 | 19 | 34 | 32 | 32 | 32 | 32 | 32 |
| 20 | **5** | **4** | **0** | **4** | **8** | **10** | 24 | 23 | 23 | 23 | 23 | 23 |

Note: Story drifts for both orthogonal directions of the building are considered. Probabilities smaller than 15% are indicated by bold font, whereas probabilities larger than 50% are indicated by italic font ($DR_{x,n} = n$th-story drift in X-direction).

rotation is to utilize the as-recorded orientation, which can be viewed as a randomly selected direction. The response from such an arbitrary orientation may be larger or smaller than the FN/FP values.

### How Often Does The Value of Response Quantity from the Arbitrary Direction Exceed that of the FN/FP Value?

The probability values presented in Table 4 provide the answer. For example, the 35% value for record Pair No. 1 and first story drift in the X-direction means that, among 5,000 trials, the response corresponding to a randomly chosen direction exceeds the FN/FP value 35% of the time. However, the latter remark is not valid for all record pairs and all response quantities, as demonstrated by the cells indicated by italic font in Table 4. For instance, the 72% value for record Pair No. 13 and first-story drift in the Y-direction means that the response corresponding to a randomly chosen direction exceeds the FN/FP value 72% of the time. Thus, the FN/FP directions are less conservative in this particular case. Nevertheless, the relatively few red cells suggests that using the larger of the FN/FP response typically, but not always, leads to a value larger than that from a randomly chosen/as-recorded direction.

### Conclusions

The current state of practice in the United States is to rotate the as-recorded pair of ground motions to the fault-normal and fault-parallel (FN/FP) directions before they are used as input for 3D RHAs of structures within 5 km of active faults. It is assumed that this approach will lead to two sets of responses that envelope the range of possible responses over all nonredundant angles of rotation. Thus, it is considered to be a conservative approach appropriate for design verification of new structures. Based on a linear-elastic computer model of a six-story instrumented structure, this study, for the first time, evaluates the relevance of using the FN/FP directions in RHAs and demonstrates its pros and cons as follows:

1. It was shown that rotated versions of the SRSS response spectra, following the ASCE/SEI-7 provisions under Section 16.1.3.2, do not vary much with rotation angle—the maximum difference observed is less than 10%. Several rotated versions of a ground motion pair can satisfy the ASCE criteria and yet provide structural responses that can vary by a factor of 2.

2. The critical angle $\theta_{cr}$ corresponding to the largest response over all possible angles varies with the ground motion pair selected and the response quantity of interest. Therefore, it is difficult to determine an optimal building orientation that maximizes demands for all EDPs before response history analyses are conducted.

3. The use of the FN/FP directions applied along the principal directions of the building almost never guarantees that the maximum response over all possible angles will be obtained. Even though it may lead to a maximum for a specific EDP, it will simultaneously be nonconservative for other EDPs. Therefore, if the performance assessment and design verification is conducted against worst-case scenarios, then bidirectional ground motions should be applied at various angles with respect to the structure's principal directions to cover all possible responses. Although this might not be a practical solution, it could still be worth doing for certain projects.

4. Treating the as-recorded direction as a randomly chosen direction, it is observed that there is more than a 50% probability that the larger response among the two FN and FP values will exceed the response corresponding to an arbitrary orientation. The latter observation is valid for most, but not all, of the record pairs and response quantities considered. Therefore, compared to no rotation at all, use of the larger response among the two values corresponding to the FN and FP directions is warranted.

Although these observations and findings are primarily applicable to buildings and ground motions with characteristics similar to those utilized in this study, they are in close agreement with those reported in Reyes and Kalkan (2013a, b), where the influence of rotation angle on several EDPs was examined in a parametric study using symmetric (torsionally stiff) and asymmetric (torsionally flexible) modern-design single-story and multistory linear-elastic and nonlinear-inelastic buildings subjected to a different set of near-fault records.

### Acknowledgments

### References

ASCE. (2010). *Minimum design loads for buildings and other structures*, *ASCE/SEI 7-10*, Reston, VA.

Athanatopoulou, A. M. (2005). "Critical orientation of three correlated seismic components." *Eng. Struct.*, 27(2), 301–312.

Bray, J., and Rodriguez-Marek, A. (2004). "Characterization of forward-directivity ground motions in the near-fault region." *Soil Dyn. Earthquake Eng.*, 24(11), 815–828.

Dudley, R. M. (1999). *Uniform central limit theorems*, Cambridge University Press, Cambridge, UK.

Fernandez-Davila, I., Comeinetti, S., and Cruz, E. F. (2000). "Considering the bi-directional effects and the seismic angle variations in building design." *Proc., 12th World Conf. on Earthquake Engineering*, Auckland, New Zealand.

Franklin, C. Y., and Volker, J. A. (1982). "Effect of various 3-D seismic input directions on inelastic building systems based on INRESB-3D-82 Computer Program." *Proc., 7th Eur. Conf. on Earthquake Engineering*.

Chopra, A. K. (2007). *Dynamics of structures: Theory and applications to equation engineering*, 2nd Ed., Prentice-Hall, Englewood Cliffs, NJ.

Goel, R. K., and Chadwell, C. (2007). *Evaluation of current nonlinear static procedures for concrete buildings using recorded strong-motion data, data interpretation rep.*, California Strong Motion Instrumentation Program (CSMIP), Dept. of Conservation, Sacramento, CA.

Goel, R. K., and Chopra, A. K. (2004). "Evaluation of modal and FEMA pushover analysis: SAC buildings." *Earthquake Spectra*, 20(1), 225–254.

Goda, K. (2012). "Comparison of peak ductility demand of inelastic SDOF systems in maximum elastic response and major principal directions." *Earthquake Spectra*, 28(1), 385–399.

International Conference for Building Officials (ICBO). (2009). *International building code*, Whittier, CA.

International Conference for Building Officials (ICBO). (2010). *California building code*, Whittier, CA.

Kalkan, E., and Kunnath, S. K. (2006). "Effects of fling-step and forward directivity on the seismic response of buildings." *Earthquake Spectra*, 22(2), 367–390.

Kalkan, E., and Kunnath, S. K. (2007). "Effective cyclic energy as a measure of seismic demand." *J. Earthquake Eng.*, 11(5), 725–751.

Kalkan, E., and Kunnath, S. K. (2008). "Relevance of absolute and relative energy content in seismic evaluation of structures." *Adv. Struct. Eng.*, 11(1), 17–34.

Kalkan, E., and Kwong, N. S. (2012). *Evaluation of fault-normal/fault-parallel directions rotated ground motions for response history analysis of an instrumented six-story building*, USGS Open-File Report 2012–1058, Menlo Park, CA, ⟨http://pubs.usgs.gov/of/2012/1058/⟩ (Sep. 21, 2013).

Khoshnoudian, F., and Poursha, M. (2004). "Responses of three dimensional buildings under bi-directional and unidirectional seismic excitations." *Proc., 13th World Conf. on Earthquake Engineering*, Mira Digital Publishing, Vancouver, Canada.

Kojic, S., Trifunac, M. D., and Anderson, J. C. (1984). *A post earthquake response analysis of the Imperial County Services building in El Centro*, *Rep. CE 84-02*, University of Southern California, Dept. of Civil Engineering, Los Angeles.

Lagaros, N. D. (2010). "Multicomponent incremental dynamic analysis considering variable incident angle." *Struct. Infrastr. Eng.*, 6(1–2), 77–94.

Lopez, O. A., Chopra, A. K., and Hernandez, J. J. (2000). "Critical response of structures to multicomponent earthquake excitation." *Earthquake Eng. Struct. Dyn.*, 29(12), 1759–1778.

Lopez, O. A., and Torres, R. (1997). "The critical angle of seismic incidence and structural response." *Earthquake Eng. Struct. Dyn.*, 26(9), 881–894.

MacRae, G. A., and Mattheis, J. (2000). "Three-dimensional steel building response to near-fault motions." *J. Struct. Eng.*, 10.1061/(ASCE)0733-9445(2000)126:1(117), 117–126.

Mavroeidis, G. P., and Papageorgiou, A. S. (2003). "A mathematical representation of near-fault ground motions." *Bull. Seismol. Soc. Am.*, 93(3), 1099–1131.

*OpenSees* [Computer software]. Berkeley, CA, ⟨http://opensees.berkeley.edu⟩ (Sep. 21, 2013).

Penzien, J., and Watabe, M. (1974). "Characteristics of 3-dimensional earthquake ground motions." *Earthquake Eng. Struct. Dyn.*, 3(4), 365–373.

Reyes, J. C., and Kalkan, E. (2013a). "Significance of rotating ground motions on behavior of symmetric- and asymmetric-plan structures: Part 1. Single-story structures." *Earthquake Spectra*, in press.

Reyes, J. C., and Kalkan, E. (2013b). "Significance of rotating ground motions on behavior of symmetric- and asymmetric-plan structures: Part 2. Multi-story structures." *Earthquake Spectra*, in press.

Rigato, A., and Medina, R. A. (2007). "Influence of angle of incidence on the seismic demands for inelastic single-storey structures subjected to bi-directional ground motions." *Eng. Struct.*, 29(10), 2593–2601.

Tezcan, S. S., and Alhan, C. (2001). "Parametric analysis of irregular structures under seismic loading according to the new Turkish Earthquake Code." *Eng. Struct.*, 23(6), 600–609.

Todorovska, M. I., and Trifunac, M. D. (2008). "Earthquake damage detection in the Imperial County Services Building. III: Analysis of wave travel times via impulse response functions." *Soil Dyn. Earthquake Eng.*, 28(5), 387–404.

Wasserman, L. (2004). *All of statistics: A concise course in statistical inference*, Springer, New York.

Wilson, E. L., Suharwardy, I., and Habibullah, A. (1995). "A clarification of the orthogonal effects in a three-dimensional seismic analysis." *Earthquake Spectra*, 11(4), 659–666.